ChemComm

COMMUNICATION

View Article Online
View Journal | View Issue

Cite this: *Chem. Commun.*, 2021, **57**, 12532

Received 1st October 2021,
Accepted 26th October 2021

DOI: 10.1039/d1cc05557g

rsc.li/chemcomm

Attempted reduction of a carbazolyl-diiodoalane†

Alexander Hinz * and Maximilian P. Müller

We report details of our attempts to reduce the bulky carbazolyl diiodoalane [R–AlI$_2$]. The reducing agents employed include KC$_8$, Cp*$_2$Co and the Mg(I) compound [(^{Mes}BDI)Mg]$_2$. The use of KC$_8$ allowed the spectroscopic observation of the alanediyl [R–Al]. With Cp*$_2$Co as the reducing agent, the alanediyl [R–Al] was obtained as a crystalline material in low yield, but paramagnetic impurities remained. When diiodoalane [R–AlI$_2$] was treated with [(^{Mes}BDI)-Mg]$_2$, no reduction but a 2 : 1 addition was observed.

Aluminium(I) chemistry has seen remarkable progress in the last few years after initial discoveries of [AlCp*]$_4$ (Scheme 1, **A**) by Schnöckel and [(^{Dipp}BDI)Al] (**B**) by Roesky.[1,2] Both compounds were utilised in further reactions, spanning both coordination chemistry and the activation of small molecules.[3–5] A new impulse was given by attempts of generating dialumenes, where Tokitoh obtained hidden examples[6,7] and Inoue succeeded in synthesising the base-stabilised dialumene (**C**).[8] Anionic aluminium nucleophiles have been in the focus of interest since the groups of Aldridge and Goicoechea reported on the first example bearing a xanthene-based diamido substituent (**D**). Later, other examples without O-donor moieties or even N-substituents were reported by Yamashita, Kinjo, Coles, Harder and Hill.[9–13] Braunschweig and coworkers utilised a bulky cyclopentadienyl derivative to stabilise the monomeric Al(I) compound **E**.[14] The quest for a genuine mono-coordinated Al(I) compound is still ongoing. The group of Power was the first to succeed when they employed the bulkiest terphenyl substituent available and prepared the alanediyl **F**.[15,16]

Our interest was directed in a similar direction, but instead of a terphenyl substituent we attempted to use the carbazole-based ligand R. After establishing a bulky carbazole (R) as the main scaffold for our endeavours in main-group chemistry, we initially investigated group 14 derivatives (Scheme 1, bottom).[17,18] These efforts lead to quasi-monocoordinate divalent cations with the general formula [R–E]$^+$ (E = Si, Ge, Sn, Pb) in salts with the weakly coordinating anion [Al(OC$_4$F$_9$)$_4$]$^-$. Subsequently, the synthesis of the isovalent electronic molecule [R–Al] was targeted, incorporating Al(I) instead of, for instance, Si(II). As recently Zhang and Liu published the synthesis of the free carbazolyl aluminylene [R–Al] and its coordination behaviour towards transition metal complexes,[19] we are prompted to disseminate our current results with respect to carbazolyl aluminium chemistry and to conclude this direction of work in our group.

Before starting any experimental work, we studied the possible decomposition pathways of the carbazolyl-bearing compound [R–Al] *in silico*. The terminal alanediyl could in principle be inserted into either of the (sp^2)C–H or (sp^2)C–C(sp^2) bonds of the flanking arenes. Both reactions would lead to minima on the energy hypersurface, among which the C–C insertion product is thermodynamically disfavoured over [R–Al] by +124.5 kJ mol^{-1}, while the C–H insertion product is favoured by −38.6 kJ mol^{-1}. In both cases, however, the activation barrier for the process is very large (C–C insertion,

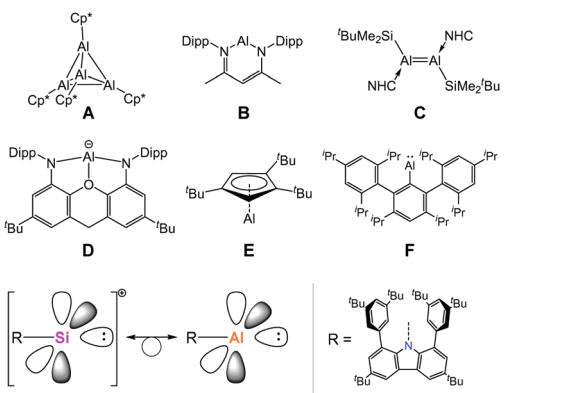

Scheme 1 Known Al(I) species and carbazolyl compounds.

Karlsruher Institut für Technologie (KIT), Institut für Anorganische Chemie (AOC), Engesserstraße 15, Karlsruhe D-76131, Germany. E-mail: alexander.hinz@kit.edu

† Electronic supplementary information (ESI) available. CCDC 2108296–2108299. For ESI and crystallographic data in CIF or other electronic format see DOI: 10.1039/d1cc05557g

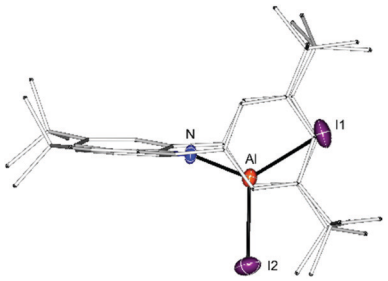

Fig. 1 Non-disordered molecular structure of [R–AlI_2] in crystals of the benzene solvate; thermal ellipsoids at 50% probability at 200 K.

280.2; C–H insertion, 248.5 kJ mol^{-1}), so it is not expected to take place under ambient conditions. This situation is comparable to the $[R–Si]^+$ cation (see the ESI,† Computational details).

With these encouraging data in hand, we initiated practical work efforts. The diiodoalane [R–AlI_2] can be prepared by metathesis of potassium carbazolide [R–K] with AlI_3 in toluene, in analogy to the preparation of carbazolyl trihalosilanes. The reaction mixture usually adopts a dark green colour, but after filtration and evaporation of the solvent this by-product can be removed by washing with *n*-hexane. [R–AlI_2] is surprisingly poorly soluble in hexane and toluene and decomposes in THF at ambient temperature within minutes, but can be crystallised from hot toluene to yield a colourless crystalline material. In these crystals obtained from the toluene solution, the AlI_2 moiety is multiply disordered (Fig. S4, ESI†). Remarkably, from a sample of [R–AlI_2] recrystallised from benzene, the solvate [R–AlI_2]·C_6H_6 could be obtained, in which no AlI_2 disorder was found (Fig. 1). In this molecular structure, the N–Al bond length amounts to 1.830(3) Å, and the Al atom possesses a short contact to one *o*-C atom of the flanking arene of 2.584(4) Å, illustrating its acidity. In solution, however, this contact is fluxional, as all NMR resonances for the aryl-^{t}Bu groups are magnetically equivalent (see the ESI† 2.1).

With [R–AlI_2] available, we made attempts to carry out reduction. The initial attempts were conducted with KC_8 as the reducing agent (Scheme 2). However, this reduction proved problematic: while diiodoalane [R–AlI_2] was reduced to [R–Al], also the alanediyl [R–Al] was reduced, and potassium carbazolide [R–K] was formed. With stepwise addition of small portions of KC_8 and waiting for the reduction to complete, a maximum spectroscopic yield of [R–Al] of 55% was obtained (Fig. S6, ESI†). From this mixture, the product [R–Al] could not be

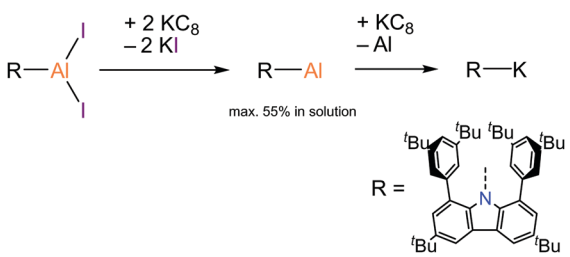

Scheme 2 Reduction of $RAlI_2$ with KC_8.

isolated. However, spectroscopic characterisation was successful. ^{1}H NMR spectra indicate C_{2v} symmetry in the product molecule, *i.e.* all *o*-^{t}Bu groups are magnetically equivalent. Furthermore, the ^{15}N NMR spectra, which showed a marked downfield shift of the carbazolyl-N resonance for the monocoordinated silicon cation $[R–Si]^+$, show a similar behaviour here. The ^{15}N NMR resonance of [R–AlI_2] at 132.8 ppm is shifted downfield by 50 ppm to 183.0 ppm upon reduction. A comparable phenomenon was observed in the deprotonation of [R–H] and the halide abstraction from [R–SiBr] yielding [R–K] and $[R–Si]^+$, respectively.[17,20] This can be rationalised by considering delocalising the lone pair of electrons at N into suitable acceptor orbitals (Fig. S14, ESI†). In [R–AlI_2] and [R–SiBr], Al and Si possess an unoccupied p orbital in the plane of the carbazole scaffold and thus orthogonal to the occupied p orbital at N, while in [R–H] no p orbital contribution is relevant at the N–H. Upon deprotonation and formation of [R–Al], $[R–Si]^+$ and [R–K], a p-type acceptor orbital becomes available and thus the N atom is magnetically deshielded. This is also mirrored in an increasing computed anisotropy of the shielding tensor and a marked change in its YY component (see the ESI† 4.2). Therefore, the ^{15}N NMR resonance also corroborates the formal coordination number 1 of the metal attached to the carbazolyl substituent in the reduction product [R–Al]. The ^{27}Al NMR shift would be even more diagnostic as it was estimated at +80 ppm by DFT methods, but could not be observed.

In another experiment, we employed Cp^*_2Co as the reducing agent. The reaction mixture immediately turned dark brown, indicating a reaction had taken place. After filtration, evaporation of the solvent, and washing, a few orange crystals were obtained. The reaction could only be carried out successfully on a very small scale, yielding only a few crystals each time. Reactions carried out on a larger scale that should have yielded several hundred milligrams of the product did not allow isolation of [R–Al] at all. Difficulties arise from ensuing paramagnetic impurities which have to be removed by crystallisation. Thus, both reducing agents show poorer performance than K/KI which was employed by Liu and allowed isolation of [R–Al] in 67% yield.[19]

The XRD data for [R–Al] showed its mono-ligated aluminium structural motif immediately after structure solution, but shows significant disorder (Fig. S11, ESI†). In the major part (Fig. 2), the metrics show a N–Al bond length of 1.908(3) Å as well as the four shortest Al–C contacts to the *o*-C atoms of the flanking arenes of 3.015(3), 3.019(3), 3.178(3) and 3.175(3) Å. These data are in agreement with computational predictions (N–Al 1.950 Å, all Al–C contacts >3 Å) and the observed results of the Liu group.[19]

In another attempt of reduction of the diiodoalane [R–AlI_2], Jones' Mg(I) compound $[(^{Mes}BDI)Mg]_2$ was employed as the reducing agent (Scheme 3),[21,22] as alanates and alane–carbene adducts are known to be reduced with this agent.[23,24] Contrary to the expectation of a 1 : 1 reaction, even in a 1 : 1 reaction mixture, 2 : 1 consumption of the starting materials was observed with complex NMR characteristics indicating a

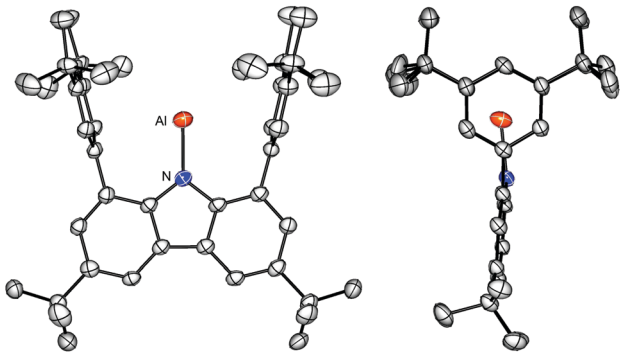

Fig. 2 Molecular structure of [R–Al]. Thermal ellipsoids at 50% probability at 150 K.

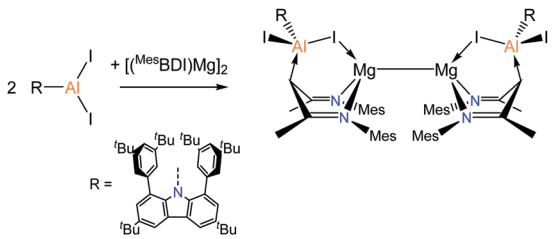

Scheme 3 Reaction of $RAlI_2$ with $[(^{Mes}BDI)Mg]_2$.

product of low symmetry with respect to the carbazole moiety. The reaction was repeated with a 2:1 stoichiometry and allowed the isolation of the orange crystalline product after filtration and concentration in 45% yield. The XRD analysis revealed that the addition of the diiodoalane across both $[(^{Mes}BDI)Mg]$ moieties of the Mg(I) starting material had taken place (Fig. 3), and thus a 2:1 reaction could occur and yield $[(RAlI_2)_2\{(^{Mes}BDI)Mg\}_2]$. This reaction left the Mg–Mg bond intact and no reduction of the alane was achieved. This reactivity differs from the literature known reactions of Mg(I) with Al(III)[23,24] because in this instance the acidity of the alane is unquenched.

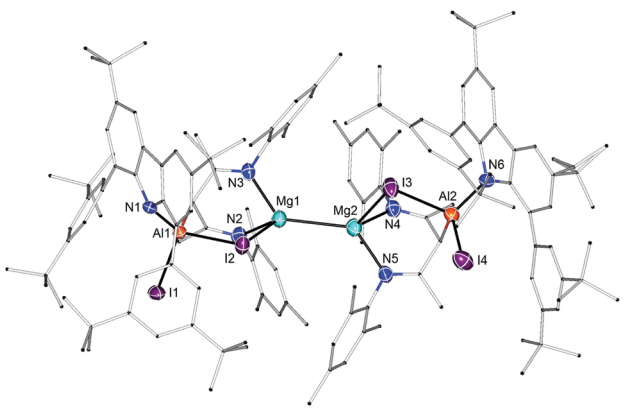

Fig. 3 Molecular structures of $[(RAlI_2)_2\{(^{Mes}BDI)Mg\}_2]$. Thermal ellipsoids at 50% probability at 110 K.

The basicity of the gamma-C atom of the BDI scaffold was demonstrated in several examples of d-block metal complexes with H^+ as the electrophile,[25–31] but was not yet observed in the class of Mg(I) compounds. However, $[\{(BDI)Mg\}_2]$ were involved in acid–base reactions, where coordination of Lewis base ethers, pyridines or carbenes was observed at the acidic Mg atoms which could also boost the reactivity.[32–34]

The molecular structure of $[(RAlI_2)_2\{(^{Mes}BDI)Mg\}_2]$ (Fig. 3) shows the Mg–Mg bond with a length of 2.851(3) Å which is nearly unchanged compared to original Mg(I) compounds (2.8457(8) Å).[21] The newly formed Al–C bonds are of 2.079(6) and 2.098(6) Å lengths, respectively. The terminal Al–I bonds with lengths of 2.521(2) and 2.505(2) Å are shorter than the respective bonds to the bridging iodides (2.608(2) and 2.592(2) Å). The Mg–I contacts are long and amount to 2.926(2) and 2.953(2) Å, which are longer than that in $[(^{Mes}BDI)MgI(OEt_2)]$ (2.6915(9) Å).[32] The NMR spectroscopic properties are consistent with the molecular structure in the crystal. There are six distinct ^{t}Bu group resonances as well six inequivalent methyl group resonances. In the ^{15}N NMR spectrum, the resonances of the BDI scaffold could be found at 257.8 and 268.4 ppm, while the carbazolyl-N NMR resonance could not be observed.

Analysis of the frontier orbitals of this compound shows a localised (s–s)σ-bond in the HOMO and a set of two quasi-degenerate unoccupied orbitals delocalised over one BDI and carbazole moiety each (Fig. 4). The HOMO energy of −4.197 eV is elevated by 0.411 eV compared to the original $[\{(^{Mes}BDI)Mg\}_2]$, while the LUMO energy is essentially unchanged. This accounts for a slightly narrower HOMO–LUMO gap in $[(RAlI_2)_2\{(^{Mes}BDI)Mg\}_2]$, and therefore it is more orange than yellow in colour. An NBO analysis of $[(RAlI_2)_2\{(^{Mes}BDI)Mg\}_2]$ shows a largely unchanged charge distribution

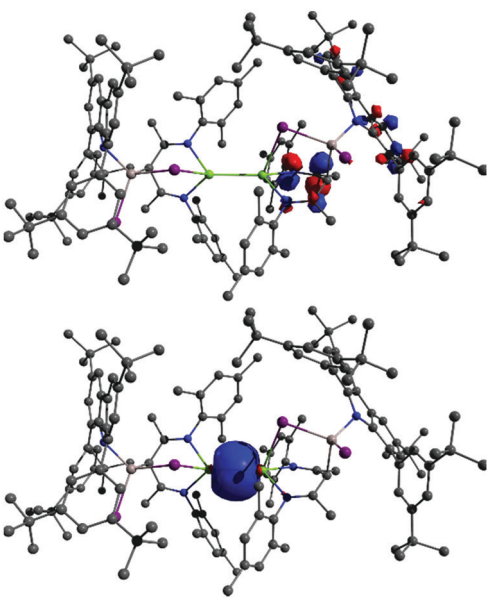

Fig. 4 Frontier orbitals of $[(RAlI_2)_2\{(^{Mes}BDI)Mg\}_2]$ (top: LUMO, bottom: HOMO).

upon adduct formation (Fig. S15, ESI†) with the largest changes observed in the NCCCN moiety of the BDI scaffold, where more negative charge is accumulated at the γ-C. The bonds involving the aluminium atoms show strongly polarised interactions, with contributions of only 14–23% of Al to the NBO σ-orbitals (ESI† 4.3). There is no NBO σ-bond between Mg and the bridging iodide, but second-order perturbation theory analysis shows several weak delocalisations of I lone pairs to Mg. Comparison of the topological characteristics of both the Al–I and Mg–I interactions shows a bond critical point, where the properties differ significantly (ESI† 4.3). Both the electron density ρ and the Laplacian $\nabla(\rho)$ show lower values for Mg–I (ρ 0.017, $\nabla(\rho)$ 0.060) than for Al–I (ρ 0.046, $\nabla(\rho)$ 0.096), indicating a weaker interaction.

We reported on the details of the application of classic reducing agents in the reaction with carbazolyl diiodoalane [R–AlI_2]. This allowed the generation and characterisation of [R–Al], but no large-scale preparations. When Mg(I) compounds were employed in the reaction, no reduction but an addition reaction was observed. This emphasises the relevance of finding suitable reducing agents in the preparation of low valent compounds.

This work was financially supported by the *Fonds der Chemischen Industrie* through a Liebig Fellowship for A. H. and a Kekule Fellowship for M. P. M. as well as by the German Research Foundation (DFG) through the Emmy Noether Programme (HI 2063/1-1). We thank Prof. Frank Breher and Prof. Peter Roesky for continuous support. This work was carried out with the support of the *Karlsruhe Nano Micro Facility* (KNMF), a Helmholtz Research Infrastructure at Karlsruhe Institute of Technology (KIT), and Prof. Dieter Fenske is gratefully acknowledged for help with XRD. We acknowledge support by the state of Baden-Württemberg through bwHPC and DFG through grant no. INST 40/467-1 FUGG (JUSTUS cluster).

Conflicts of interest

There are no conflicts to declare.

Notes and references

1 C. Dohmeier, C. Robl, M. Tacke and H. Schnöckel, *Angew. Chem., Int. Ed. Engl.*, 1991, **30**, 564–565.
2 C. Cui, H. W. Roesky, H. Schmidt, M. Noltemeyer, H. Hao and F. Cimpoesu, *Angew. Chem.*, 2000, **39**, 4274–4276.
3 M. T. Gamer, P. W. Roesky, S. N. Konchenko, P. Nava and R. Ahlrichs, *Angew. Chem., Int. Ed.*, 2006, **45**, 4447–4451.
4 G. He, O. Shynkaruk, M. W. Lui and E. Rivard, *Chem. Rev.*, 2014, **114**, 7815–7880.
5 T. Chu and G. I. Nikonov, *Chem. Rev.*, 2018, **118**, 3608–3680.
6 T. Agou, K. Nagata and N. Tokitoh, *Angew. Chem., Int. Ed.*, 2013, **52**, 10818–10821.
7 K. Nagata, T. Murosaki, T. Agou, T. Sasamori, T. Matsuo and N. Tokitoh, *Angew. Chem., Int. Ed.*, 2016, 1–5.
8 P. Bag, A. Porzelt, P. J. Altmann and S. Inoue, *J. Am. Chem. Soc.*, 2017, **139**, 14384–14387.
9 J. Hicks, P. Vasko, J. M. Goicoechea and S. Aldridge, *Nature*, 2018, **557**, 92–95.
10 S. Kurumada, S. Takamori and M. Yamashita, *Nat. Chem.*, 2019, **12**, 10–13.
11 K. Koshino and R. Kinjo, *J. Am. Chem. Soc.*, 2020, **142**, 9057–9062.
12 R. J. Schwamm, M. P. Coles, M. S. Hill, M. F. Mahon, C. L. McMullin, N. A. Rajabi and A. S. S. Wilson, *Angew. Chem., Int. Ed.*, 2020, **59**, 3928–3932.
13 S. Grams, J. Eyselein, J. Langer, C. Färber and S. Harder, *Angew. Chem.*, 2020, **132**, 16116–16120.
14 A. Hofmann, T. Tröster, T. Kupfer and H. Braunschweig, *Chem. Sci.*, 2019, **10**, 3421–3428.
15 J. D. Queen, A. Lehmann, J. C. Fettinger, H. M. Tuononen and P. P. Power, *J. Am. Chem. Soc.*, 2020, **142**, 20554–20559.
16 J. D. Queen, S. Irvankoski, J. C. Fettinger, H. M. Tuononen and P. P. Power, *J. Am. Chem. Soc.*, 2021, **143**, 6351–6356.
17 A. Hinz, *Chem. – Eur. J.*, 2019, **25**, 3267–3271.
18 A. Hinz, *Angew. Chem., Int. Ed.*, 2020, **59**, 19065–19069.
19 X. Zhang and L. L. Liu, *Angew. Chem., Int. Ed.*, 2021, DOI: 10.1002/anie.202111975.
20 A. Hinz, *Angew. Chem., Int. Ed.*, 2020, **59**, 19065–19069.
21 S. P. Green, C. Jones and A. Stasch, *Science*, 2007, **318**, 1754–1757.
22 J. Hicks, M. Juckel, A. Paparo, D. Dange and C. Jones, *Organometallics*, 2018, **37**, 4810–4813.
23 S. J. Bonyhady, D. Collis, G. Frenking, N. Holzmann, C. Jones and A. Stasch, *Nat. Chem.*, 2010, **2**, 865–869.
24 C. Jones, *Nat. Rev. Chem.*, 2017, **1**, 0059.
25 C. Camp and J. Arnold, *Dalton Trans.*, 2016, **45**, 14462–14498.
26 D. W. Shaffer, S. A. Ryken, R. A. Zarkesh and A. F. Heyduk, *Inorg. Chem.*, 2012, **51**, 12122–12131.
27 G. Bai, P. Wei, A. Das and D. W. Stephan, *Organometallics*, 2006, **25**, 5870–5878.
28 A. Hadzovic, J. Janetzko and D. Song, *Dalton Trans.*, 2008, 3279–3281.
29 D. F. Schreiber, C. O'Connor, C. Grave, H. Müller-Bunz, R. Scopelliti, P. J. Dyson and A. D. Phillips, *Organometallics*, 2013, **32**, 7345–7356.
30 A. Venugopal, M. K. Ghosh, H. Jürgens, K. W. Törnroos, O. Swang, M. Tilset and R. H. Heyn, *Organometallics*, 2010, **29**, 2248–2253.
31 C. Camp, L. Maron, R. G. Bergman and J. Arnold, *J. Am. Chem. Soc.*, 2014, **136**, 17652–17661.
32 S. J. Bonyhady, C. Jones, S. Nembenna, A. Stasch, A. J. Edwards and G. J. McIntyre, *Chem. – Eur. J.*, 2010, **16**, 938–955.
33 K. Yuvaraj, I. Douair, D. D. L. Jones, L. Maron and C. Jones, *Chem. Sci.*, 2020, **11**, 3516–3522.
34 K. Yuvaraj, I. Douair, A. Paparo, L. Maron and C. Jones, *J. Am. Chem. Soc.*, 2019, **141**, 8764–8768.